

## **Supplementary Material**

### **Metal-ion binding by humic substances as emergent functions of labile supramolecular assemblies**

Elena A. Vialykh,<sup>A,E</sup> Dennis R. Salahub<sup>B,C</sup> and Gopal Achari<sup>D</sup>

<sup>A</sup>Department of Chemistry, University of Calgary, 2500 University Dr. NW, Calgary, Alberta, Canada, T2N 1N4.

<sup>B</sup>Department of Chemistry, Centre for Molecular Simulation (CMS), Institute for Quantum Science and Technology and Quantum Alberta (IQST), University of Calgary, 2500 University Drive NW, Calgary, Alberta, Canada, T2N 1N4.

<sup>C</sup>College of Chemistry and Chemical Engineering, Henan University of Technology, 100 Lian Hua Street, High-Tech Development Zone, Zhengzhou 450001, China.

<sup>D</sup>Schulich School of Engineering, University of Calgary, 2500 University Dr. NW, Calgary, Alberta, Canada, T2N 1N4.

<sup>E</sup>Corresponding author. Email: [elena.vialykh@ucalgary.ca](mailto:elena.vialykh@ucalgary.ca)

## Table of Contents

Text S1. The guidelines for the selection of molecules to generate models

Table S1. Composition of three systems generated for computational modeling.

Text S2. Description of the ReaxFF force field

Text S3. Hydrogen bonding, hydrophobic/hydrophilic surface area, potential energy and Me ion complexation analysis

Table S2. The average percentage of oxygen groups directly bound to Me ion with respect to the total number of each group in the model.

Table S3. Average binding energy ( $\Delta E$ , kcal/mol) of Cu-Ligand complexes

Table S4. Binding energy ( $\Delta E$ , kcal/mol) of Mg-Ligand complexes and bonds

Table S5. Number of H-bonds formed in the models after MD simulations under various conditions

Table S6. Radius of gyration ( $\text{\AA}$ ) of the organic models after MD simulations under various conditions.

Table S7. Hydrophilic surface area ( $\text{\AA}^2$ ) of the models after MD simulations under various conditions

Table S8. Hydrophobic surface area ( $\text{\AA}^2$ ) of the models after MD simulations under various conditions

Text S1. The guidelines for the selection of molecules to generate models

The guidelines for the choice of molecules were adequate fits: to elemental composition; NMR-derived functional group distribution and aromatic-to-aliphatic, and ‘carbohydrate like’ ratios. The molecular mass distribution is close to values from FT-ICR MS 100-700 Da for SRFA, with a bias toward formulas reported from the high-resolution MS studies.

The first system, SRFA-22, was built by using molecular fragments identified by FT-ICR MS and Orbitrap MS analysis (Remucal et al. 2012) with the addition of 3 carbohydrate moieties to generate a better representation of NMR spectra. Out of 172 identified fragments the most abundant 10 fragments were chosen in a way that the overall chemical characteristics fit to average parameters of SRFA, that is, the reference sample provided by IHSS (SI Table S2). The molecular weights of fragments varied between 110 and 400 Da.

Molecular fragments for the second model, SRFA-6, were selected from the structures proposed by Leenheer et al. (1994). These hypothetical structures were designed by integrating state-of-the-art knowledge from analytical data on SRFA. The main difference from the previous system was in the size of the molecular fragments, though the molecular weight of the system overall was similar. The third system, SRHA-6, was created by modifying molecular fragments of the second system so that overall it fits average SRHA characteristics. However, the molecular fragment sizes remained similar to the SRFA-6 model and varied between 660 and 840 Da.

Leenheer et al. (1994) used the following characteristics of SRFA to generate models:

1. Number-average molecular weight.
2. Elemental contents corrected for moisture and ash contents:
  - Carbon (C)
  - Hydrogen (H)
  - Oxygen (O)
  - Nitrogen (N)
  - Sulfur (S)
  - Phosphorus (P)
3. Average molecular formula.
4. Average moles of unsaturation ( $\phi$ ).
5. Carbon distribution by type of carbon:
  - Aliphatic
  - H-C-O (alcohol, ether, ester, acetal, ketal)
  - O-C-O (acetal, ketal) plus aromatic
  - Aromatic
  - Phenols, phenolic esters, aromatic ethers
  - Carboxyl plus ester
  - Ketone
6. Hydrogen distribution:
  - Exchangeable-hydrogen distribution by type of hydrogen:

Carboxyl

Phenol

Alcohol

Nonexchangeable hydrogen distribution by type of hydrogen:

Isolated aliphatic

$\text{H}_3\text{C}-\text{C}=\text{O}$ ,  $\text{H}_2\text{C}-\text{C}=\text{O}$ ,  $\text{H}-\text{C}-\text{C}=\text{O}$ ,  $\text{H}_3-\text{C}-\phi$ ,  $\text{H}_2-\text{C}-\phi$ ,  $\text{H}-\text{C}-\phi$ ,  $\text{H}-\text{C}-\text{O}$ ,  $\text{H}-\phi$

7. Oxygen distribution by type of oxygen:

Carboxyl

Ester

Carboxyl+ester

Ketone

Phenol

Alcohol

Acetal and ketal

Ether

8. Amino acids

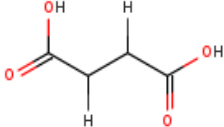
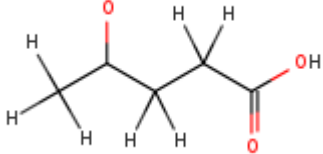
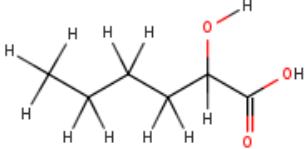
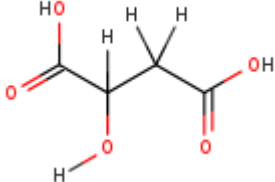
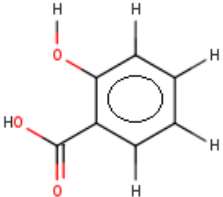
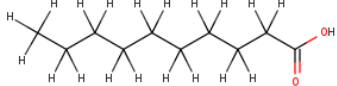
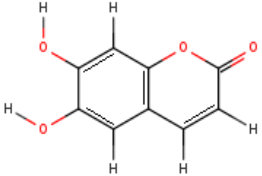
Metal-binding sites, nitrogencontaining functional groups

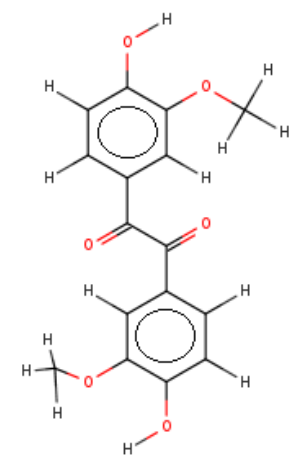
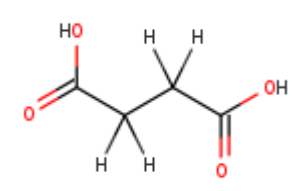
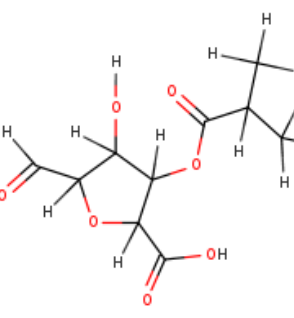
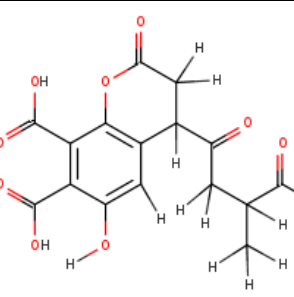
Metal-binding sites, sulfurcontaining functional groups

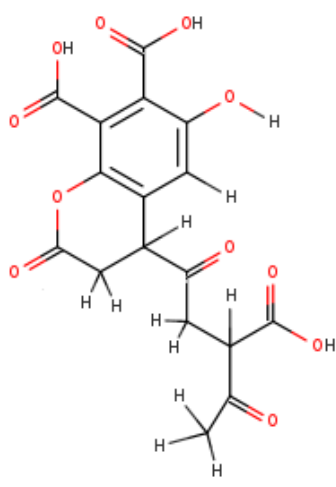
9. Organic free radicals

10. Metal-binding sites

Table S1. Composition of three systems generated for computational modeling.

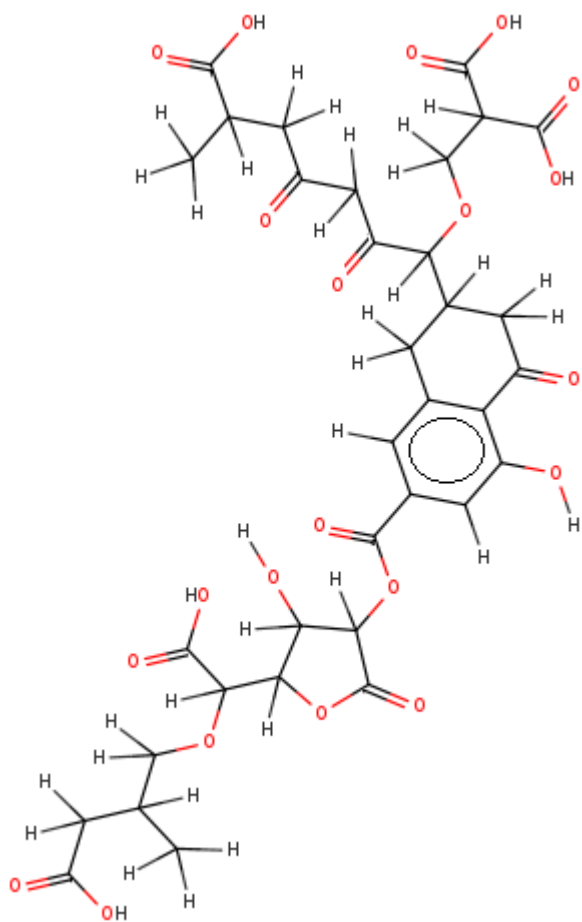
SRFA-22								
N of molecules	Chemical formula	Carbonyl	Carboxyl	Ester	Aromatic	Hetero aliphatic	Aliphatic	Chemical structure
2	$C_4H_4O_4$	0	2	0	2	0	0	
3	$C_5H_8O_3$	1	1	0	0	0	3	
3	$C_6H_{12}O_3$	0	1	0	0	1	4	
2	$C_4H_6O_5$	0	2	0	0	1	1	
1	$C_7H_6O_3$	0	1	0	6	0	0	
1	$C_{10}H_{20}O_2$	0	1	0	0	0	9	
1	$C_9H_6O_4$	0	0	1	9	0	0	

1	$C_{16}H_{14}O_6$	2	0	0	12	2	0	
2	$C_4H_6O_4$	0	2	0	0	0	2	
3	$C_{10}H_{14}O_7$	0	1	1	0	5	3	
1	$C_{16}H_{14}O_{10}$	1	3	1	6	0	5	

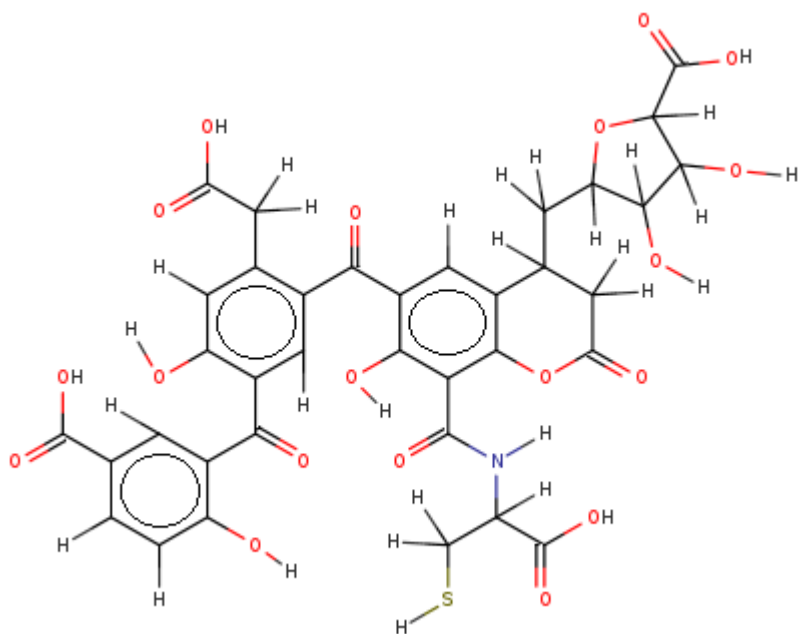
2	C <sub>17</sub> H <sub>14</sub> O <sub>11</sub>	2	3	1	6	0	5	
Functional group concentration mmol/g (% of carbon/total carbon)		2.48 (5.6)	7.94 (17.9)	1.74 (3.9)	12.2 (27.4)	5.46 (12.3)	14.9 (33.5)	

SRFA-6								
N of molecules	Chemical formula	Carbonyl	Carboxyl	Ester	Aromatic	Acetal	Heteroaliphatic	Aliphatic
1	C <sub>34</sub> H <sub>38</sub> O <sub>21</sub>	3	5	2	6	0	7	11
1	C <sub>37</sub> H <sub>44</sub> O <sub>22</sub>	2	6	2	6	1	4	16
1	C <sub>35</sub> H <sub>43</sub> O <sub>21</sub> N	3	3	3	6	3	5	12
1	C <sub>33</sub> H <sub>37</sub> O <sub>16</sub> N	2	4	2	10	0	4	11
1	C <sub>31</sub> H <sub>30</sub> O <sub>19</sub>	2	6	2	10	0	1	10
1	C <sub>33</sub> H <sub>35</sub> O <sub>17</sub> N S	2	4	2	12	0	6	7
Functional group concentration mmol/g (% of carbon/total carbon)		3.15 (6.9)	6.30 (13.8)	2.92 (6.4)	11.24 (24.6)	0.90 (2.0)	6.07 (13.3)	15.1 (33.0)
SRHA-6								
N of molecules	Chemical formula	Carbonyl	Carboxyl	Ester	Aromatic	Acetal	Heteroaliphatic	Aliphatic
2	C <sub>33</sub> H <sub>32</sub> O <sub>19</sub>	2	4	2	12	1	4	8
1	C <sub>38</sub> H <sub>43</sub> O <sub>19</sub> N	2	4	2	12	1	6	11
1	C <sub>31</sub> H <sub>31</sub> O <sub>16</sub> N	2	3	2	12	0	4	8
1	C <sub>31</sub> H <sub>25</sub> O <sub>16</sub> N	2	3	2	15	0	1	7
1	C <sub>36</sub> H <sub>31</sub> O <sub>19</sub> N S	2	3	1	18	0	6	4
Functional group concentration mmol/g (% of carbon/total carbon)		2.78 (6.0)	4.86 (10.4)	2.54 (5.5)	18.7 (40.1)	0.69 (1.5)	5.78 (12.4)	10.6 (22.8)

A molecular fragments from SRFA-6



A molecular fragments from SRHA-6



## Text S2. Description of the ReaxFF force field

ReaxFF is a reactive force field that was used to simulate the various interactions, including 1) all connectivity-dependent interactions (i.e. valence and torsion angles) are made bond-order dependent, ensuring that their energy contributions disappear upon bond dissociation; 2) nonbonded interactions (van der Waals, Coulomb) are calculated between every atom pair, irrespective of connectivity. Excessive close-range nonbonded interactions are avoided by shielding; 3) ReaxFF uses a geometry-dependent charge calculation scheme that accounts for polarization effects. The force field is trained against a QM-derived set of energies for small molecules and clusters. For each element, several parameters to describe valence bond parameters, electronegativity, hardness, and other effects are optimized to reproduce the QM derived energies and charges. The electron equilibration method (EEM) is implemented to derive the changing atomic charges. This formulation enables polarization and charge transfer effects.

The main advantage of ReaxFF is its ability to simulate covalent bond formation and breaking, i.e. primary chemical reactions of organic molecules. ReaxFF force field parameters are optimized to reproduce a suitable reference organic data set, derived mainly via quantum chemical calculations (QC) and compared to a number of QM/MM calculations (for more details please see (Monti et al. 2013)). Being empirical in nature, ReaxFF allows MD simulations of large reactive chemical systems (1000s of atoms) and yet retains an accuracy close to QC.

The ReaxFF water model is used to simulate aqueous solutions with explicit solvent. The parameters for the water model (molecule) are determined from quantum mechanics.

Since the HS of focus here consists of organic molecules in an aqueous environment, we used the ReaxFF potential developed to simulate biomolecules (Monti et al. 2013). In the Vialykh et al. Environmental Chemistry, 2019, ReaxFF was tested for its ability to simulate molecular interactions that are important for complex organic mixtures and that occur in HS, including a) H-bonding, (b) hydrophobic interactions, c)  $\pi$ -stacking, d) charge transfer complexation, e) labile metal-ion complexation, and f) chemical reactions between molecular fragments. ReaxFF was used to study the functional behaviour of three different systems with organic contaminants, phenol, toluene and benzene, in the vacuum and aqueous phase, as well as complexation with  $\text{Cu}^{2+}$  in vacuum. A detailed description of the ReaxFF force field is presented in Vialykh et al. Environmental Chemistry, 2019 and includes the following:

In 2001 van Duin et al. (2001) developed a new force field (ReaxFF). The main advantage of ReaxFF is its ability to simulate covalent bond formation and breaking, i.e. primary chemical reactions of organic molecules. The general equation used in ReaxFF is:

$$E_{system} = E_{bond} + E_{over} + E_{under} + E_{lp} + E_{val} + E_{tor} + E_{wdWaals} + E_{Coulomb} \quad (1)$$

It takes into account partial contributions to the total system potential energy ( $E_{system}$ ) related to the bond ( $E_{bond}$ ), over-coordination penalty ( $E_{over}$ ) and under-coordination stability ( $E_{under}$ ), lone pair ( $E_{lp}$ ), valence angle ( $E_{val}$ ) and torsion ( $E_{tor}$ ), and non-bonding Coulombic ( $E_{Coulomb}$ ) and van der Waals ( $E_{wdWaals}$ ) energies, respectively (Russo and van Duin 2011).

The main assumption used in ReaxFF is that bond order ( $BO_{ij}$ ) can be derived directly from

interatomic distance ( $r_{ij}$ ) according to equation (2):

$$BO'_{il} = \exp\left[p_{bo,1} * \left(\frac{r_{ij}}{r_0}\right)^{p_{bo,2}}\right] + \exp\left[p_{bo,3} * \left(\frac{r_{ij}}{r_0}\right)^{p_{bo,4}}\right] + \exp\left[p_{bo,5} * \left(\frac{r_{ij}}{r_0}\right)^{p_{bo,6}}\right] \quad (2),$$

where  $r_0$  is the bonding equilibrium distance. Three exponential terms used in equation (2) describe: 1) the sigma bond ( $p_{bo,1}$  and  $p_{bo,2}$ ) which is unity below  $\sim 1.5$  Å but negligible above  $\sim 2.5$  Å; 2) the first pi bond ( $p_{bo,3}$  and  $p_{bo,4}$ ) which is unity below  $\sim 1.2$  Å and negligible above  $\sim 1.75$  Å, and 3) the second pi bond ( $p_{bo,5}$  and  $p_{bo,6}$ ) which is unity below  $\sim 1.0$  Å and negligible above  $\sim 1.4$  Å. As result a carbon-carbon bond has a maximum bond order of 3. For carbon-hydrogen and hydrogen-hydrogen bonds, only the sigma-bond contribution is considered, resulting in a maximum bond order of 1. The use of two main relationships, bond distance/ bond order on the one hand and bond order/ bond energy on the other, allows modeling of bond dissociation and formation with ReaxFF.

The terms  $E_{over}$ ,  $E_{under}$ ,  $E_{lp}$  are used to adjust bond order over-/under-coordination happening due to long-range interactions. When a carbon has a weak attraction/bond order with its second nearest neighbor, hydrogen atoms, this type of bonding will cause unrealistic behavior while modeling intact molecules, and must be corrected. In other words when a carbon atom has a bond order of 4 or more, these types of long-range interactions need to be negated and thus the small bond orders involving this carbon are significantly reduced to minimize their effects. Conversely, when a carbon atom has less than its optimal 4 bonds, these types of weak interactions should be allowed, so the weak bond orders are essentially unchanged. Consequently, these corrections allow accurate modeling of long-range radical attraction between atoms from different molecules as well as the realistic interactions between a radical site and its second nearest neighbors within the same molecule.

Since the bond orders are combined with functions of valence coordinates such as bond angles and torsion angles (equation 3) so that the energy contributions from bonding terms go to zero smoothly as bonds break.

$$E_{val} = [1 - \exp(\lambda * BO_1^3)] * [1 - \exp(\lambda * BO_2^3)] * \{k_a - k_b * \exp(-k_b * (\phi - \phi_0)^2)\} \quad (3),$$

where  $BO_1$  and  $BO_2$  are the bond orders for each of the two bonds connecting the three atoms within an angle.  $\lambda$  is an angular parameter set to obtain agreement with quantum calculated values,  $k_a$  and  $k_b$  are the harmonic force constants that determine the depth and width of the angular potential, respectively,  $\phi$  is the angle, and  $\phi_0$  is the equilibrium angle.

ReaxFF also allows the calculation of the polarization of charges within molecules (eq. 4):

$$\frac{\partial E}{\partial q_n} = \chi_n + 2 * q_n * \eta_n + C * \sum_{j=1} \frac{q_j}{\left\{r_{nj}^3 + \left(\frac{1}{\gamma_{nj}}\right)^3\right\}^{1/3}}, \quad (4).$$

In equation (4)  $\chi_n$  is the electronegativity and  $\eta_n$  is the hardness of element  $n$  and  $\gamma_{nj}$  is a shielding parameter between atoms  $n$  and  $j$ . The charge values are dependent on the system geometry and determined for each time step of the simulation. ReaxFF uses a geometry-dependent charge calculation scheme that accounts for polarization effects.

The van der Waals and Coulomb forces are included from the beginning and calculated (eq. 5) between every atom pair which allows the description of non-bonded interactions between all atoms.

$$E_{Coulomb} = C * \left[ \frac{q_i * q_j}{\left\{ r_{ij}^3 + \left( \frac{1}{\gamma_{ij}} \right)^3 \right\}^{1/3}} \right] \quad (5),$$

where  $q_i$  and  $q_j$  are the charges of the two atoms,  $r_{ij}$  is the interatomic distance and  $C$  is the electric constant, and  $\gamma_{ij}$  is the shielding parameter between atoms  $i$  and  $j$ .

Parameters for the dissociation and reaction curves are derived from quantum chemical calculations, thus ReaxFF allows molecular dynamics simulations of large-scale reactive chemical systems (1000s of atoms) with resulting accuracy similar to quantum mechanically based methods. Each element is represented by only 1 atom type in the force field; the force field should be able to determine equilibrium bond lengths, valence angles etc. from the chemical environment.

Text S3. Hydrogen bonding, hydrophobic/hydrophilic surface area, potential energy and Me ion complexation analysis.

The VMD tool for hydrogen bond analysis (Humphrey et al. 1996) was used to estimate the number of hydrogen bonds in the organic mixture. A hydrogen bond was considered to be formed between an atom with a hydrogen (the donor, D) and another, mainly O, atom (the acceptor, A) provided that the distance D-A is less than the cut-off distance, 3.0 Å and the angle D-H-A is less than the cut-off angle, 20° (Gumbart 2007). Radius of gyration was calculated by using VMD software ('VMD User's Guide' 2014). Chems sketch software (Hunter 1997) was used to draw 2D structures of molecules. Hydrophilic/phobic surfaces were determined according to the procedure described by (Aristilde and Sposito 2010) by using the Maestro 11 software ("Maestro 11 | Schrödinger"). The potential energy and charge of the atoms at each snapshot were calculated by ReaxFF. A Me ion was considered to form an inner/outer sphere complex if the distance between the oxygen of the binding group and the Me ion was in the range 1.5-2.5 Å/3.5-5.0 Å, respectively (which were the ranges for the two major peaks of the Me-O radial distribution function).

Table S2. The average percentage of oxygen groups directly bound to Me ion with respect to the total number of each group in the model.

	SRFA-22		SRHA-6	
	Cu <sup>2+</sup>	Mg <sup>2+</sup>	Cu <sup>2+</sup>	Mg <sup>2+</sup>
Carboxyl	33.1	22.4	20.1	38.1
Ketone	19.2	12.5	11.8	18.1
Ester	25.0	13.9	9.0	12.2
Hydroxyl	3.0	3.0	2.7	2.7

**Table S3.** Average binding energy ( $\Delta E$ , kcal/mol) of Cu-Ligand complexes.

	SRFA-22		SRFA-6		SRHA-6	
	$\Delta E$ , kcal/mol	Sd	$\Delta E$ , kcal/mol	Sd	$\Delta E$ , kcal/mol	Sd
4 organic oxygens	214.8	1.8	180.9*			
3 organic oxygens	154.4	6.5	150.6	8.7	130.9	9.8
2 organic oxygens	122.3	4.8	112.3	3.7	108.6	6.5
2 organic oxygens	111.5**					
2 organic oxygens	107.1***					
Aliphatic acid	66.2	3.5	67.4	6.5	69.1	0.8
Benzoic acid	70.0	4.8	70.3	5.7	70.6	4.5
Keton	53.2	4.4				
Ester	56.1	4.4	56.6	5.8	62.6	3.2
Phenol	65.6	1.8				

\* - non planar;

\*\* - bidentate complex with R-Ar-COO<sup>-</sup>

\*\*\* - bidentate complex with R-(CH<sub>2</sub>)<sub>n</sub>-COO<sup>-</sup>

Table S4. Binding energy ( $\Delta E$ , kcal/mol) of Mg-Ligand complexes and bonds.

	SRFA-22		SRFA-6		SRHA-6	
	$\Delta E$ , kcal/mol	Sd	$\Delta E$ , kcal/mol	Sd	$\Delta E$ , kcal/mol	Sd
4 organic oxygens			233.3	5.9	228.8	
3 organic oxygens	193.3	6.4	196.7	6.8	194.9	4.7
2 organic oxygens	136.2	2.9	148.8	3.1	140.8	3.6
2 organic oxygens *	147.0				176.3	
2 organic oxygens **					177.4	
Aliphatic acid	95.5	2.1	97.2	9.2	95.8	2.8
Benzoic acid	121.0	5.5	123.1 (90.4) ***	4.2	122.3 (103.5)	
Keton	77.2	4.9				
Ester	81.6	4.9			82.0	1.0
Phenol	90.7					
Carboxyl. double	118.78	6.1	135.24	6.9	129.58	4.7

\* - bidentate complex with R-Ar-COO<sup>-</sup>

\*\* - bidentate complex with R-(CH<sub>2</sub>)<sub>n</sub>-COO<sup>-</sup>

\*\*\* - the binding energy in brackets is for Me-COO<sup>-</sup> complex with hetroaromatic ring

**Table S5.** Number of H-bonds formed in the models after MD simulations under various conditions.

	Cu <sup>2+</sup>			Mg <sup>2+</sup>		
<b>SRFA-22</b>	<b>1</b>	<b>8</b>	<b>16</b>	<b>1</b>	<b>8</b>	<b>16</b>
1000	5.3	6.0	10.6	6.2	6.4	7.5
500	6.4	6.0	9.2	7.3	7.3	7.8
200	9.1	10.0	10.7	11.3	10.9	10.8
100	13.0	10.7	8.2	10.5	10.7	12.2
<b>SRFA-6</b>	<b>1</b>	<b>7</b>	<b>14</b>	<b>1</b>	<b>7</b>	<b>14</b>
1000	7.8	8.7	7.8	8.8	8.5	8.8
500	9.5	7.5	8.0	9.1	8.4	8.5
200	11.0	9.3	7.0	9.2	8.8	9.45
100	7.6	7.0	6.2	11.1	11.0	11.6
<b>SRHA-6</b>	<b>1</b>	<b>5</b>	<b>11</b>	<b>1</b>	<b>5</b>	<b>11</b>
1000	5.7	6.0	7.0	7.3	6.7	5.4
500	6.7	7.0	9.0	7.0	7.6	5.9
200	5.7	6.0	6.0	8.3	7.8	5.2
100	6.8	5.5	4.9	6.4	5.4	3.6

(SD for each value varies between 0.1 and 0.6)

**Table S6.** Radius of gyration (Å) of the organic models after MD simulations under various conditions.

	Cu <sup>2+</sup>			Mg <sup>2+</sup>		
	1	8	16	1	8	16
<b>SRFA-22</b>						
1000	14.62	14.32	13.41	14.80	14.65	13.62
500	12.82	12.23	12.23	13.04	12.19	12.15
200	11.15	11.04	10.69	10.15	10.20	10.36
100	9.94	10.10	10.16	9.97	10.00	9.51
<b>SRFA-6</b>						
1000	13.86	13.49	12.12	14.14	13.03	12.82
500	13.42	12.19	11.98	13.69	12.97	12.23
200	11.10	10.81	10.75	10.38	10.00	10.00
100	10.90	10.30	10.08	11.16	10.56	10.15
<b>SRHA-6</b>						
1000	12.32	12.14	12.11	12.16	11.96	11.87
500	12.42	12.02	11.52	11.74	11.70	11.23
200	11.47	11.40	11.10	10.43	10.51	9.94
100	11.07	10.18	9.64	10.21	10.38	10.36

(SD ≤ 0.15 Å for each value)

**Table S7.** Hydrophilic surface area ( $\text{\AA}^2$ ) of the models after MD simulations under various conditions.

	$\text{Cu}^{2+}$			$\text{Mg}^{2+}$		
<b>SRFA-22 (initial size of the surface <math>2087 \text{\AA}^2</math>)</b>	<b>1</b>	<b>8</b>	<b>16</b>	<b>1</b>	<b>8</b>	<b>16</b>
1000	1832	1799	1707	1670	1655	1696
500	1765	1690	1632	1615	1585	1526
200	1694	1629	1453	1617	1526	1395
100	1355	1344	1362	1556	1418	1184
<b>SRFA-6 (initial size of the surface <math>1736 \text{\AA}^2</math>)</b>	<b>1</b>	<b>7</b>	<b>14</b>	<b>1</b>	<b>7</b>	<b>14</b>
1000	1649	1579	1545	1527	1500	1458
500	1495	1475	1446	1492	1475	1440
200	1510	1492	1475	1475	1418	1415
100	1425	1336	1302	1440	1391	1363
<b>SRHA-6 (initial size of the surface <math>1503 \text{\AA}^2</math>)</b>	<b>1</b>	<b>5</b>	<b>11</b>	<b>1</b>	<b>5</b>	<b>11</b>
1000	1348	1233	1294	1346	1348	1295
500	1424	1284	1232	1373	1303	1279
200	1391	1332	1308	1345	1327	1307
100	1302	1322	1263	1152	1241	1487

(SD for each value varies between 10 and  $25 \text{\AA}^2$ )

**Table S8.** Hydrophobic surface area (Å<sup>2</sup>) of the models after MD simulations under various conditions.

	Cu <sup>2+</sup>			Mg <sup>2+</sup>		
	1	8	16	1	8	16
<b>SRFA-22 (initial size of the surface 299 Å<sup>2</sup>)</b>						
1000	495	505	532	455	491	457
500	594	601	609	592	616	613
200	716	661	561	588	577	584
100	532	550	562	499	503	603
<b>SRFA-6 (initial size of the surface 649 Å<sup>2</sup>)</b>						
1000	720	740	660	640	680	710
500	740	758	785	662	674	822
200	753	718	714	732	680	694
100	715	714	701	673	659	639
<b>SRHA-6 (initial size of the surface 792 Å<sup>2</sup>)</b>						
1000	867	961	916	896	793	844
500	1000	893	782	810	902	716
200	877	831	828	816	747	787
100	809	779	632	675	667	645

### References (Supplementary Material)

- Aristilde, L., Sposito, G., 2010. Binding of ciprofloxacin by humic substances: A molecular dynamics study. *Environ. Toxicol. Chem.* **29**, 90–98. <https://doi.org/10.1002/etc.19>
- van Duin, A.C.T., Dasgupta, S., Lorant, F., Goddard, W.A., 2001. ReaxFF: A Reactive Force Field for Hydrocarbons. *J. Phys. Chem. A* **105**, 9396–9409. <https://doi.org/10.1021/jp004368u>
- Gumbart, J.C., 2007. HBonds Plugin, Version 1.2. URL <http://www.ks.uiuc.edu/Research/vmd/plugins/hbonds/> (accessed 12.11.17).
- Humphrey, W., Dalke, A., Schulten, K., 1996. VMD: visual molecular dynamics. *J. Mol. Graph.* **14**, 33–38.
- Hunter, A.D., 1997. ACD/ChemSketch 1.0 (freeware); ACD/ChemSketch 2.0 and its Tautomers, Dictionary, and 3D Plug-ins; ACD/HNMR 2.0; ACD/CNMR 2.0. *J. Chem. Educ.* **8**, 905–906.
- Leenheer, J.A., McKnight, D.M., Thurman, E.M., MacCarthy, P., 1994. Structural Components and Proposed Structural Models of Fulvic Acid from the Suwannee River. In 'Humic Substances in the Suwannee River, Georgia: Interactions, Properties, and Proposed Structures' US

- Geological Survey, No 87-557' (Eds. Averett, R.C., Leenheer, J.A., McKnight, D.M., Thorn, K.A.). U.S. G.P.O. ; U.S. Geological Survey, Map Distribution, pp. 195–212.
- Maestro 11 | Schrödinger. URL <https://www.schrodinger.com/maestro> (accessed 12.11.17).
- Monti, S., Corozzi, A., Fristrup, P., Joshi, K.L., Shin, Y.K., Oelschlaeger, P., van Duin, A.C.T., Barone, V., 2013. Exploring the conformational and reactive dynamics of biomolecules in solution using an extended version of the glycine reactive force field. *Phys. Chem. Chem. Phys.* **15**, 15062–15077. <https://doi.org/10.1039/c3cp51931g>
- Remucal, C.K., Cory, R.M., Sander, M., McNeill, K., 2012. Low Molecular Weight Components in an Aquatic Humic Substance As Characterized by Membrane Dialysis and Orbitrap Mass Spectrometry. *Environ. Sci. Technol.* **46**, 9350–9359. <https://doi.org/10.1021/es302468q>
- Russo, M.F., van Duin, A.C.T., 2011. Atomistic-scale simulations of chemical reactions: Bridging from quantum chemistry to engineering. *Nucl. Instrum. Methods Phys. Res. Sect. B Beam Interact. Mater. At.* **269**, 1549–1554. <https://doi.org/10.1016/j.nimb.2010.12.053>
- VMD User's Guide, 2014. URL <https://www.ks.uiuc.edu/Research/vmd/vmd-1.9.2/ug.pdf> (accessed 6.20.19).